

International Atomic Energy Agency

INDC(CCP)-243/L

INDC

INTERNATIONAL NUCLEAR DATA COMMITTEE

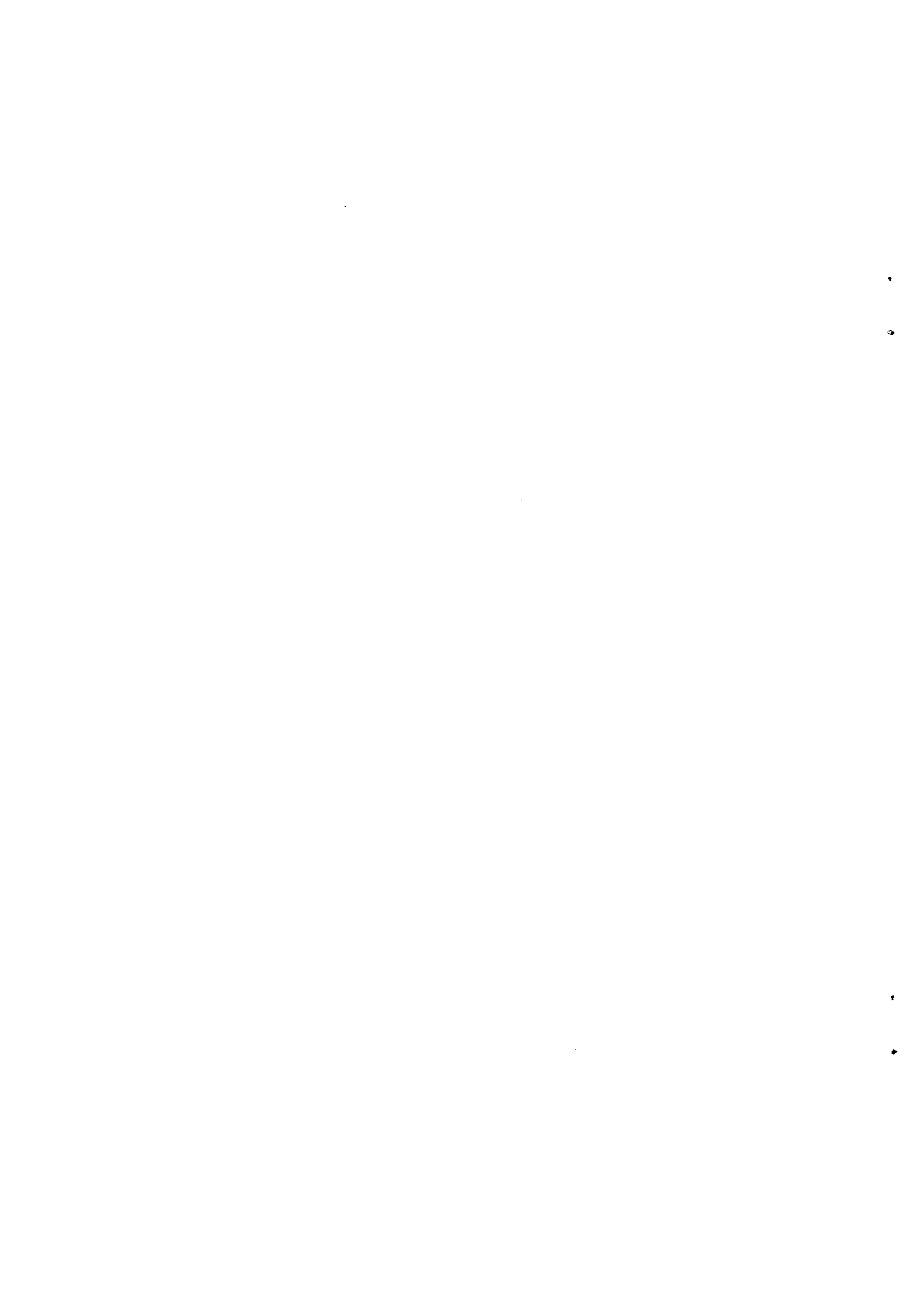
ENERGY DEPENDENCE OF THE REMOVAL CROSS-SECTION
IN PLANE LAYERS OF IRON SHIELDING

J. Jordanova, K. Ilieva, B. Khristov and G. Vojkov

Translated by the IAEA

July 1985

IAEA NUCLEAR DATA SECTION, WAGRAMERSTRASSE 5, A-1400 VIENNA



ENERGY DEPENDENCE OF THE REMOVAL CROSS-SECTION
IN PLANE LAYERS OF IRON SHIELDING

J. Jordanova, K. Ilieva, B. Khristov and G. Vojkov

Translated by the IAEA

July 1985

Reproduced by the IAEA in Austria
July 1985

85-03515

ENERGY DEPENDENCE OF THE REMOVAL CROSS-SECTION
IN PLANE LAYERS OF IRON SHIELDING

J. Jordanova, K. Ilieva, B. Khristov and G. Vojkov

Semi-empirical methods based on what is called the removal cross-section Σ_{rem} are widely used for high-speed evaluation of fast neutron fluxes and the doses they deliver. Determination of this quantity is based on an approximation of the decay of the fast neutron flux beyond a layer of shielding material with an exponential function, namely:

$$\phi(d, E_{trs}) = S e^{-d \Sigma_{rem}(E_{trs})} \quad (1)$$

where S is the intensity of the source, d is the thickness of the shielding layer, E_{trs} is the threshold energy of the detector (in the sense of the lower boundary of the interval over which the neutron flux is considered).

Contemporary literature offers only a very limited quantity of such data^{1/}, and what is more, they suffer from obvious inconsistencies due mainly to differences in geometry and the method of detection, which are unfortunately not always described by the authors. In this sense the removal cross-section method is not always dependable. It is therefore important that when such data are derived an indication of their applicability is given.

In our study the data were obtained for the removal cross-section Σ_{rem} and the relaxation length λ_{rel}^{-1} in the case of neutron flux from a 14 MeV one-directional source passing through layers of iron shielding. The numerical computations of the neutron distributions were performed by the discrete ordinate transport technique (ANISN [4]) and the Monte Carlo method (MORSE [5]) in a 25-group approximation for the energy dependence of the neutron flux. Since in the absence of light elements, the concept of removal cross-section can only be applied to energy levels of up to 3-4 MeV [1, 2] in our study only that component of the flow which penetrates rapidly was evaluated.

Table 1 shows the decay of the neutron flux L after passing through iron shieldings of various thicknesses d (the thicknesses are given in the first line). Also shown is the width of the energy intervals over which the neutron flux was evaluated, which makes it possible to compare the results of the measurements using various threshold detectors.

^{1/} The small amount of data on Σ_{rem} is explained by the fact that the relevant computations or measurements are complex and time-consuming.

Table 1. Neutron flux attenuation constants L(cm) behind Fe barriers of varying width d

Energy interval MeV	d = 4 cm	d = 6 cm	d = 8 cm	d = 10 cm	d = 12 cm
------------------------	----------	----------	----------	-----------	-----------

See original for figures

As can be seen from Table 1 and also from Fig. 1, the decay of the neutron flux after passing through barriers with a thickness of $l \sim 3/\lambda_t$ (where λ_t is the free path length of 14 MeV neutrons) is more or less constant, i.e. the removal cross-section concept can be applied. The fast neutron flux after the barrier can then be described by expression (1), where $\Sigma_{rem} = L^{-1}$.

Table 2 gives data for the removal cross-section and relaxation length in the case of an iron medium. These data were obtained by us^{2/} as well as other authors. Let us look at them in more detail.

In the first few lines Σ_{rem} is given for various values of the lower boundary of the energy interval E_{trs} ^{3/}. As was to be expected, a reduction in the lower limit of E_{trs} is matched by a reduction in Σ_{rem} , i.e. the fastest neutrons are those which are attenuated most quickly. Moreover, our analysis revealed the following interesting empirical interdependency between the removal cross-section and the lower boundary of the energy interval, namely:

$$\Sigma_{rem} = \Sigma_t(14 \text{ MeV}) [\alpha + \beta E_{trs} (\text{MeV})] \quad (2)$$

where Σ_t is the total macroscopic cross-section at $E = 14.9$ MeV, $\alpha = 0.471 \pm 0.004$; $\beta = 0.0104 \pm 0.0005$.

This dependence, found by the least squares method, makes it possible to determine the removal cross-section for a neutron flux emitted by a 14 MeV source in the 14.9-4.0 MeV energy interval by means of the total cross-section Σ_t and threshold energy E_{trs} with a <2% margin of error.

Lower down, Table 2 presents the data we obtained for the relaxation length^{4/} of the fast neutron flux evaluated over a 10-12 cm interval of space in layers of varying thickness: 12, 60 and 100 cm. These data were derived for the purpose of comparison with the results obtained by other authors, though also in order to test the assertion, frequently encountered in the literature, that Σ_{rem} and λ_{rel}^{-1} are identical (see for example /6,7/).

^{2/} The error which affects our data is only due to approximating the flow by an exponential function. Its smallness confirms the applicability of the removal cross-section method.

^{3/} It should be noted that authors do not always give information on the lower boundary of the energy interval for which Σ_{rem} has been evaluated. This complicates the corresponding comparisons and applications.

^{4/} Let us bear in mind that the relaxation length is a constant for exponential decay of the neutron flux in an "infinite" medium.

▶ Table 2. Removal cross-section Σ_{rem} and relaxation length λ_{rel} for iron

Energy interval (MeV)	Σ_{rem} or λ_{rel}^{-1} (cm ⁻¹)	L or λ_{rel} (cm)	σ_{rem} (barn)	$\delta = \frac{\Sigma_{rem}}{\Sigma_t(14 \text{ MeV})}$	Method of obtaining results
1	2	3	4	5	6
See original for figures					Our computation (ANISN) for barriers of thicknesses up to 12 cm
					Our computation (MORSE) for barriers of up to 12 cm; unit size 40 x 40 cm
					Our computation (ANISN) for a 12 cm thick layer
					Our computation (ANISN) for a 60 cm thick layer
					Our computation (ANISN) for a 100 cm thick layer
					[6] With a threshold detector
					[7] With a threshold detector

[1] page 114

[7] page 80

[1] page 132, with a layer
of light moderator before
the Fe layer

[1] page 132, with a layer
of light moderator before
the Fe layer

[1] page 118, Table 5.5 with
a B₄C (10-12 cm) moderator;
detector ²³²Th(n, f)

[3] with water in front of
the Fe layer (5 cm);
detector ⁶³Cu(n, 2n)⁶²Cu,
page 175

[3] with water in front of
the Fe layer (15-20 cm);
detector ²³²Th(n, f)
page 175

[3] with water in front of
the Fe layer (65 cm);
detector BF₃, page 175

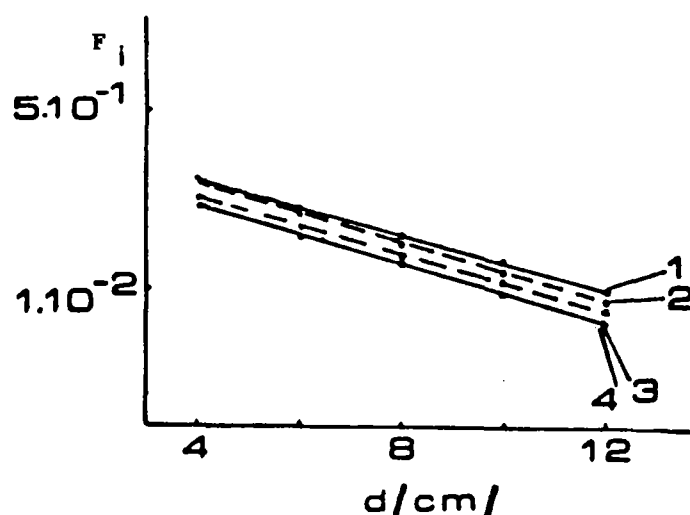


Fig. 1. Attenuation of the neutron flux behind barriers of various thicknesses over different energy intervals:

- | | |
|------------------|-------------------|
| 1-/14.9-4.0/MeV; | 2-/14.9-5.0/MeV; |
| 3-/14.9-8.2/MeV; | 4-/14.9-12.2/MeV. |

Comparison of the results for λ_{rel}^{-1} with the removal cross-section Σ_{rem} for barrier geometry (up to 12 cm) shows that treating these values as identical is only valid in cases where λ_{rel} is evaluated (measured) in the /0-12/ cm range in an infinite medium (60-100 cm). The maximum error, given threshold energy of 4 MeV, is then of the order of 7%, which appears satisfactory for the high-speed method. If the medium is not "infinite" enough (e.g. 12 cm, as is the case in Refs 6 and 7), the assumption of such identity is valid only in cases of high threshold energy (more than 10 MeV), while for a threshold energy of 4 MeV, Σ_{rem} and λ_{rel}^{-1} diverge by 30%.

The calculations were carried out using the MORSE three-dimensional program and allow for the finite dimensions of the source - a disc of 5 cm radius and a barrier of 40 x 40 cm. The source is simulated by the random sampling method.

The discrepancies between the data obtained by us and by other authors point to the influence of the geometrical conditions and detection method (threshold energy). Moreover the data presented indicate that $\Sigma_{rem} = \lambda_{rel}^{-1}$ only in a few instances, so that caution must be observed in treating them as identical.

REFERENCES

1. Biological protection of moveable reactor facilities, (Ed. Broder) Atomizdat, Moscow (1969).
2. BERGEL'SON, B.R., SUVOROV, A.P., TORLIN, B.Z., Multigroup methods of computing protection from neutrons, Atomizdat, Moscow (1970).
3. KAZANSKIJ, Yu.A., et al., Physical studies on reactor shielding, Atomizdat, Moscow (1966).
4. ANISN-W Code. One-Dimensional Discrete Ordinate Transport Technique. WANL-PR-(LL)-034, Vol. IV (1970).
5. EMMET, M.B., The MORSE Monte Carlo Transport Code System, ORNL. 4972 (Feb. 1975).
6. Utilization of Neutron Generators. IAEA, Laboratory Manual, Debrecen (1982).
7. COPPER, P.N., KABIR, S.M., J. Nuclear Energy 26 (1972) p. 569.
8. VOYKOV, G., GADJOKOV, V., MINCHEV, S., L26P3S34, INDC(BUL) - 007/GV, Vienna (March 1983).

THRESHOLD ENERGY DEPENDENCE OF REMOVAL CROSS-SECTION FOR A
UNIDIRECTIONAL AND ISOTROPIC SOURCE OF 14 MeV NEUTRONS

J. Jordanova, K. Ilieva, N. Sokolinova and V. Khristov

The semi-empirical removal cross-section method is widely used for the evaluation of neutron radiation behind layers. According to this method, the fast neutron component (up to 4 MeV) is approximated by an exponential function with an attenuation constant, which is the so-called removal cross-section Σ_{rem} . As can be seen from the proceedings of the 6th Radiation Safety International Congress (RSIC) [1], in addition to the two- and three-dimensional methods of evaluating the shielding of nuclear facilities, the refinement of semi-empirical methods continues, as these require less computer time.

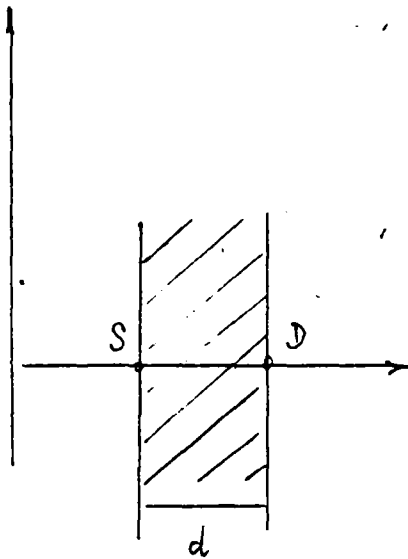
This paper accordingly presents data on removal cross-section as a function of the threshold energy of detection^{1/} for a monoenergetic and monodirectional (along the measurement axis) and isotropic 14 MeV source.

The authors of Refs [2] and [3] compared the results of our experiments with their own computations, and also with the results of other authors. These results and comparisons lead to the following conclusions. Removal cross-section data depend to a large extent on the geometrical conditions in which they are evaluated. Furthermore, a simple linear dependence was discovered between the removal cross-section and the total macroscopic cross-section for 14 MeV neutrons Σ_t and the threshold detection energy E_{trs} . It was further demonstrated that taking the finite dimensions of the source and the shielding layer into account (using the MORSE program), when the lateral dimensions of the barrier are greater than $\delta\lambda_t$ (λ_t being the mean free path of the 14 MeV neutrons in the shielding) does not contribute anything of any value, so that one-dimensional analysis using the discrete ordinate method (ANISN) is perfectly satisfactory. It should also be noted that the numerical and experimental results match each other well (see Table 1(a), (b), and (c)[3]), thereby confirming the accuracy of our results on the basis of numerical computations.

In the work we are describing, the removal cross-sections for the basic shielding materials (aluminium, iron, copper and lead) were obtained using numerically^{2/} derived neutron fluxes which had passed through barriers (1-3) λ_t in thickness.

1/ The arbitrarily selected lower boundary of the energy interval over which the flux is evaluated.

2/ The ANISN code [4] and the 25-group library L26P3S34 [5] were used for the computation.



Geometrical arrangement of source S and detector D behind a barrier of thickness d.

The geometry of the problem is shown in Fig. 1. A monodirectional or isotropic 14 MeV source is placed in front of the barrier. The detector is located immediately behind the barrier. The theoretical flux beyond the barrier is a function of the layer thickness and is contrasted with the empirical dependence.

$$\Phi(d, E_{trs}) = \int e^{-\Sigma_{rem}(E_{trs})} \quad (1)$$

where in the general case $S = S_0 B$ is a source of fast neutrons in which the accumulation of delayed neutrons (S_0 being the initial source of 14 MeV neutrons) is allowed for by means of the coefficient B. If the source is monodirectional, then $B = 1$. The values of the constant for an isotropic source are given in Table 1.

Tables 2 - 5 give the values of the neutron flux attenuation constants L after a barrier with a thickness of $(1-3) \lambda_t$, the macroscopic removal cross-sections $\Sigma_{rem} = L^{-1}$, the microscopic removal cross-sections $\sigma_{rem} = \Sigma_{rem}/N$ (where N is the density of the element in atoms/cm³), and the relationship $\sigma = \Sigma_{rem}/\Sigma_t$ (14 MeV). The error indicated is due to the exponential approximation.

In the case of a monodirectional source the data on the constant show that the approximation adopted $[6] \Sigma_{rem} = 0.6 \Sigma_t$ for elements with atomic numbers $Z = >18$ is a very rough one and occurs, moreover, where the energy threshold is very high ($E > 12$ MeV); in the case of lower thres-

Table 1. Coefficient of accumulation B for an isotropic source

Energy Interval MeV	Al	Fe	Cu	Pb
14.9-12.2	0.705	0.715	0.685	0.705
14.9-10.0	0.725	0.731	0.697	0.714
14.9-8.2	0.735	0.740	0.703	0.720
14.9-5.0	0.767	0.778	0.721	0.737
14.9-4.0	0.776	0.803	0.728	0.751

holds the values of δ , as can be seen from the results obtained, are much smaller. Where aluminium was the shielding material, the values of δ we obtained matched the proposed approximation $\Sigma_{rem} = 0.76\Sigma_t$ for elements from $11 \leq Z \leq 18$, likewise for the first energy boundary only.

In the case of isotropic sources, as was to be expected, the removal cross-sections are greater than the values for a monodirectional source, owing to the greater angular spread of the initial flux.

The energy dependence σ_{rem} on E_{trs} ($E_{trs} > 4$ MeV) can be well described by the linear function

$$\sigma_{rem} = \sigma_t (14 \text{ MeV}) [\alpha + \beta E (\text{MeV})] \quad (2)$$

The values of the parameters α and β are presented in Table 6. The error due to the linear approximation is less than 1% for the α coefficient, and 4.5% for the β coefficient.

Table 2. Aluminium barrier shielding $\Sigma_t(14 \text{ MeV}) = 0.1047$; $N = 0.0603 \text{ at}\cdot\text{cm}^{-3}$

Energy Interval MeV	Unidirectional source				Isotropic source			
	L (cm)	$\Sigma_{\text{rem}} (\text{cm}^{-1})$	$\sigma_{\text{rem}} (\text{barn})$	$\delta = \frac{\Sigma_{\text{rem}}}{\Sigma_t(14 \text{ MeV})}$	L (cm)	$\Sigma_{\text{rem}} (\text{cm}^{-1})$	$\sigma_{\text{rem}} (\text{barn})$	$\delta = \frac{\Sigma_{\text{rem}}}{\Sigma_t(14 \text{ MeV})}$
See original for figures								

Table 3. Iron barrier shielding $\Sigma_t(14 \text{ MeV}) = 0.2264$; $N = 0.0849 \text{ at}\cdot\text{cm}^{-3}$

Energy Interval MeV	Unidirectional source ^{1/}				Isotropic source			
	L (cm)	$\Sigma_{\text{rem}} (\text{cm}^{-1})$	$\sigma_{\text{rem}} (\text{barn})$	$\delta = \frac{\Sigma_{\text{rem}}}{\Sigma_t(14 \text{ MeV})}$	L (cm)	$\Sigma_{\text{rem}} (\text{cm}^{-1})$	$\sigma_{\text{rem}} (\text{barn})$	$\delta = \frac{\Sigma_{\text{rem}}}{\Sigma_t(14 \text{ MeV})}$
See original for figures								

^{1/} These data were obtained in reference [3].

Table 4. Copper barrier shielding $\Sigma_t(14 \text{ MeV}) = 0.2577$; $N = 0.0847 \text{ at}\cdot\text{cm}^3$

Energy Interval MeV	Unidirectional source				Isotropic source			
	L (cm)	$\Sigma_{\text{rem}} (\text{cm}^{-1})$	$\sigma_{\text{rem}} (\text{barn})$	$\delta = \frac{\Sigma_{\text{rem}}}{\Sigma_t(14 \text{ MeV})}$	L (cm)	$\Sigma_{\text{rem}} (\text{cm}^{-1})$	$\sigma_{\text{rem}} (\text{barn})$	$\delta = \frac{\Sigma_{\text{rem}}}{\Sigma_t(14 \text{ MeV})}$

See original for figures

Table 5. Lead barrier shielding $\Sigma_t(14 \text{ MeV}) = 0.1772$; $N = 0.03348 \text{ at}\cdot\text{cm}^3$

Energy Interval MeV	Unidirectional source				Isotropic source			
	L (cm)	$\Sigma_{\text{rem}} (\text{cm}^{-1})$	$\sigma_{\text{rem}} (\text{barn})$	$\delta = \frac{\Sigma_{\text{rem}}}{\Sigma_t(14 \text{ MeV})}$	L (cm)	$\Sigma_{\text{rem}} (\text{cm}^{-1})$	$\sigma_{\text{rem}} (\text{barn})$	$\delta = \frac{\Sigma_{\text{rem}}}{\Sigma_t(14 \text{ MeV})}$

See original for figures

Table 6.

Element	Unidirectional source		Isotropic source	
	α	β	α	β
Al	0.59	0.0130	0.83	0.020
Fe	0.47	0.010	0.73	0.011
Cu	0.49	0.0053	0.71	0.004
Pb	0.45	0.007	0.70	0.007

REFERENCES

1. RSIC Newsletter, ORNL (April 1983) p. 3, (August 1983) p. 2.
2. JORDANOVA, J., ILIEVA, K., KHRISTOV, V., VOJKOV, G., Energy dependence of removal cross-section in flat layers of iron shielding, Duke. Ban, No. 3 (1984) (in press).
3. JORDANOVA, J., ILIEVA, K., KHRISTOV, V., TROSHEV, T., SOKOLINOVA, N., PENCHEV, O., 14 MeV neutron removal cross-section for shielding media of aluminium, iron, copper and lead, item No. 3 (1984) (in press).
4. ANISN-W Code. One-Dimensional Discrete Ordinate Transport Technique. WANL-PR-(LL)-034, Vol. IV (1970).
5. VOJKOV, G., GADJOKOV, V., MINCHEV, S., L26P3S34, INDC(BUL) - 007/GV, Vienna (March 1983).
6. Utilization of Neutron Generators. IAEA, Laboratory Manual Debrecen (1982).